Journal of Communications and Information Networks
Vol.1, No.2, Aug. 2016
DOI: 10.11959/j.issn.2096-1081.2016.034

Research paper

Channel measurement and modeling for the 15-GHz radio band in an indoor corridor environment

XU Hui[1,2,3], ZHANG Wuxiong[1,2,3], YANG Yang[1,2,3]

1. Key Lab of Wireless Sensor Network and Communication, Chinese Academy of Sciences, Shanghai 200050, China
2. Shanghai Institute of Microsystem and Information Technology, Chinese Academy of Sciences, Shanghai 200050, China
3. Shanghai Research Center for Wireless Communications, Shanghai 201210, China

Abstract: Traditional mobile communication systems mainly work on the licensed frequency band near or below 3 GHz; however, this band is becoming increasingly crowded. On the other hand, there are abundant unlicensed spectrum resources in higher frequency bands, e.g., 6 GHz, 15 GHz, and 28 GHz, and if those bands are applied, the current spectrum shortage problem could be effectively alleviated. However, the wireless channel characteristics and models are important but still unknown, and thus in this study, extensive measurements and modeling have been conducted to study the characteristics of the high-frequency 15-GHz band. Specifically, a PN(Pseudo Noise) sequence based time-domain measurement system was built and applied to measure the propagation characteristics of the LOS (Line-of-Sight) and NLOS (Non-Line-of-Sight) scenarios in an indoor corridor at 15 GHz. Then, in-depth analysis and modeling on the large-scale characteristics of wireless channels, the relationship between distance and path loss, the path loss exponent, and the shadow fading standard variance are provided. Moreover, the relationship between received power and different elevation angles was studied. In the measurement, two 25-dBi horn antennas with a 10 half-power beam width are used to change elevation angles in the transmitting terminal and azimuth angles in the receiving terminal for all measurement points. The findings and results in this work will serve as a reference and basis for future theoretical studies of the 15-GHz band.

Key words: 5G mobile network, 15 GHz, high frequency, channel measurement, channel modeling

Citation: XU H, ZHANG W X, YANG Y. Channel measurement and modeling for the 15-GHz radio band in an indoor corridor environment[J]. Journal of communications and information networks, 2016, 1(2): 102-108.

1 Introduction

With continuous development of mobile communication networks, spectrum resources become crowded. High-frequency spectrum resources can effectively alleviate the current shortage of spectrum resources, achieving short-range communication at high speed to meet the capacity and trans-mission rate requirements of 5G communications. A sufficient amount of available bandwidth, miniaturized antennas and devices, and higher antenna gain are the advantages of mobile communication in high-

Manuscript received Aug. 4, 2016; accepted Aug. 18, 2016
This research is partially supported by The National High Technology Research Development Program of China (863 Program) (No.2014AA01A706), The National Natural Science Foundation of China (No.61471346), The National Science and Technology Major Project (No.2014ZX03003012), The Science and Technology Commission of Shanghai Municipality (No.14DZ2281000).

frequency, millimeter-wave radio. The application of the high frequency band to mobile communication is a future development trend and a high concern in the industry[1]. With the rapid development of mobile communication services, people in office buildings, supermarkets, conference rooms, and other places need to transmit voice, video, and other data, thus the communication quality in the indoor scenario has attracted increasing attention. Because the propagation characteristics of indoor wireless channels influences and even decides the communication process and result, research on indoor radio wave propagation is of great significance. Indeed, there have been many studies regarding measurement and analysis of the indoor channel[2-9]. The 60-GHz indoor channel characteristics, such as RMS Root-Mean-Square delay spread, delay spread characteristics, and power delay profile, were studied in[2-5]. The path loss and delay spread characteristics of indoor scenarios at 2.4 GHz and 60 GHz were also compared[6-8]. The path loss statistical model of UWB (Ultra-WideBand) signals was researched in residential environments[9]. In addition, outdoor high-frequency channel model research has also been carried out. Researchers have conducted a study of the 28-GHz millimeter-wave channel model in dense urban N-LOS scenarios[10]. Researchers described the broadband channel measurement at 17 GHz and studied the important parameters of the channel, such as RMS delay spread, path loss factor, and their statistical characteristics[11]. 2G and 3G communication have occupied most of the spectra below 2 GHz, which are the most suitable spectra for the development of mobile communication; the other available spectra are increasingly dispersed. It is difficult to find a suitable complete spectrum between 3 GHz and 6 GHz because of the uniqueness of spectrum resources and the historical heritage regarding the use and distribution of spectrum. On the contrary, in the 6-GHz to 15-GHz band, there are many spectrum resources that can be used for mobile communication and have not been fully developed. At present, wireless channel measurement and modeling studies in the 15-GHz frequency band are rare. In our project, time-domain channel measurement based on a PN sequence was used to measure the propagation channel in indoor LOS and NLOS scenarios at 15 GHz, and the large-scale characteristics of the channel were analyzed. Although for 5G millimeter-wave communication, 28 GHz, 39 GHz, and 73 GHz are excellent candidates for the frequency band, the 15-GHz frequency band is also a good option for its low path loss and wide bandwidth, both in indoor and outdoor environments. The rest of this paper is organized as follows. In Section 2, we introduce the measurement system, measurement environment, and measurement method. The data processing and corresponding results are presented in Section 3. Section 4 summarizes this work.

2 Measurement method and scenario

2.1 Measurement method

Broadband channel measurement can be conducted in the time domain to obtain the impulse response, or in the frequency-domain to obtain the frequency response. Frequency domain channel measurement uses the frequency sweeping method and takes a long time for each measurement, and thus may result in difficulty in distinguishing the useful signal from noise, whereas the timedomain measurement will not have this problem. Therefore, we used a time-domain channel measurement system based on a PN sequence. At the transmitting terminal, the PRBS11 sequence generated by a PN generator was modulated by BPSK after filtering by a square-root raised cosine filter, and the filtered signals were transmitted out by a horn antenna. The data processing was

the reverse of this process. In our measurement, an AWG (Arbitrary Waveform Generator), PSG (vector signal generator), PSA (vector signal analyzer), and mixed-signal OSC (OSCilloscopes) were used. Unlike traditional channel measurement methods, which use a trigger signal to connect the PSG and PSA with the capability to analyze signals with a bandwidth no more than 160 MHz, in this work, the bandwidth under measurement was 500 MHz, and thus we connected the PSG with the OSC, which is a more powerful approach. At the transmitter side, the IQ modulation bandwidth of AWG and PSG is up to 2 GHz, and the OSC bandwidth is up to 8 GHz. The AWG had two independent channels to generate the I and Q signals. The PSG up-converted the IQ signals to a specified frequency. At the receiver side, the PXA was used to down-convert the signal in a specified frequency to an IF (Intermediate-Frequency) signal, and the OSC was responsible for collecting data. The antennas used in the measurement were standard horn antennas with a 10° HPBW (Half-Power Beam Width) and 25-dBi gain. In the measurement, we used the AWG to generate a trigger signal to ensure synchronization between the transmitter and receiver. The azimuth angle was in the range 0° to 360°, and the elevation angle was in the range from −45° to 45°. The transmitter and the receiver used the same antenna. The measurement system block diagram is shown in Fig.1.

In our measurement, we used the sliding correlation measurement method and made full use of the self-correlation properties of the PN sequence. The transmitter transmitted the modulated PN sequence signal, and the received signal was stored in the computer after high-speed sampling, and then correlated with the same PN sequence as in the transmitter to obtain the time-domain channel characteristics. First, at the transmitting terminal, the AWG generated the baseband IQ signals, and the IQ signals were amplified by a high-power amplifier after up-conversion by the PSG; the amplified signals were then transmitted by the horn antenna. At the receiving terminal, the received signals were processed by a low-noise amplifier and then down-converted by the signal analyzer to obtain the IF signals. The IF signals were collected by the OSC according to sample number or time to obtain the IQ data. The related parameters are shown in Tab.1.

Table 1 Measurement parameter configuration

frequency	14.8 GHz
RF bandwidth	500 MHz
Tx power	0 dBm
antenna HPBW	Tx/Rx: 10°
antenna gain	25 dBi
antenna height	Tx/Rx: 1.08 m
two-axis turntable	horizontal: 0°~360°; vertical: −45°~45°

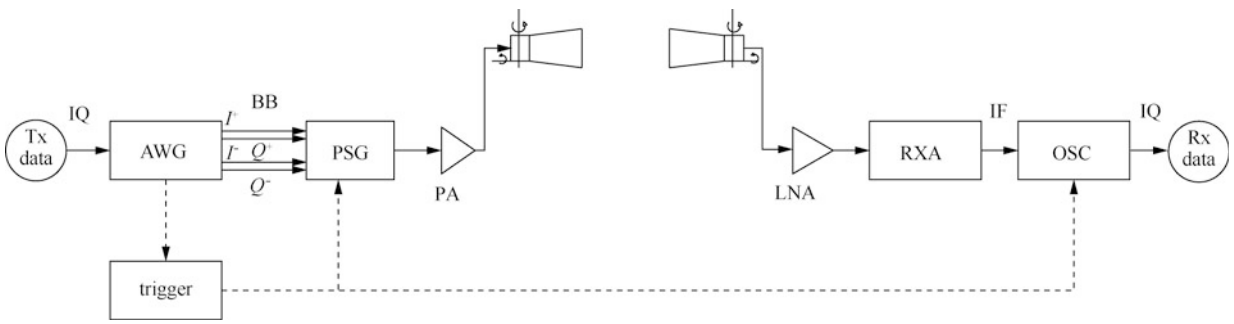

Figure 1 Measurement system block diagram

2.2 Measurement scenario and configuration

Our measurements were carried out in LOS and NLOS scenarios in a corridor environment. The transmitter and re-ceiver locations are shown in Fig.2. In the LOS measurement, the transmitter and receiver were both in the middle of the corridor. In order to analyze the relationship between received power and the angles, we rotated the antenna in the measuring process. For each measurement point, the antenna elevation angle changed from −5° to 0° to 5°, and for each elevation angle, the receiving antenna azimuth angle rotated from 0° and 360° in 5° steps. Therefore, for each point, a total of 219 measurements were carried out. We measured at eight adjacent points in all, with an interval of 6 m. The receiver was stationary, and the transmitter moved in the middle of the corridor. In the NLOS measurement, the receiver was moved to the corner and the transmitter moved the same as in the LOS measurement, as shown in Fig.2. The transmitting antenna and receiving antenna rotation were the same as those in the LOS measurement. The measurements were carried out in a typical corridor environment; the corridor was 51 m long, 2 m wide, 2.5 m high, and 5.2 m wide around the corner. Both sides of the corridor featured concrete walls and wooden office doors. In the experiment, the transmitting and receiving antennas were at the same height, and the transmitter and receiver were in equal status. The real environment and the plan are shown in Tab.2.

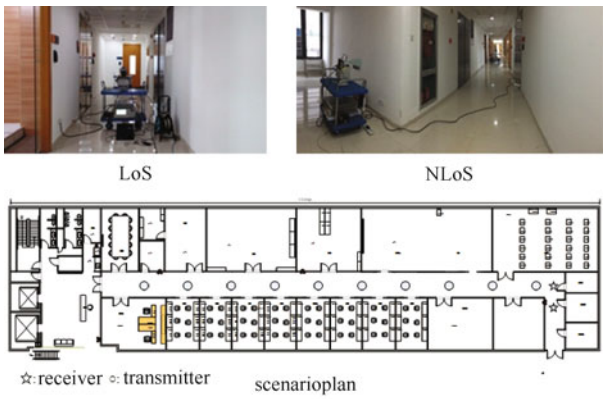

Figure 2 Measurement scenarios

The measurement configurations are shown in Tab.2. Through the proposed measurement system and method, we can obtain the received I and Q data. We used the PN sequence to slide correlate with the I and Q data, and then squared the result to obtain the PDP (Power Delay Profile).

3 Data processing method and analysis

3.1 Data processing method

According to the measurement system, we adopted the processing method shown in Fig.3. First, the IQ data were downsampled after convolution with the filter parameter, and then slide correlated with the PN sequence to obtain the PDP.

We obtained the absolute received power through the PDP, and thus we obtained path loss under different transmitting elevation angles and different receiving azimuth angles for each measurement point.

Table 2 Measurement configuration

parameter	LOS	NLOS
Tx moving range	1~48 m	6 m, 12 m
Rx moving range	stationary	stationary
Tx vertical rotationangle of the antenna	−5°, 0°, 5°	0°
Rx horizontal rotationangle of the antenna	0°~360° with 5° per rotation	0°~360° with 5° per rotation

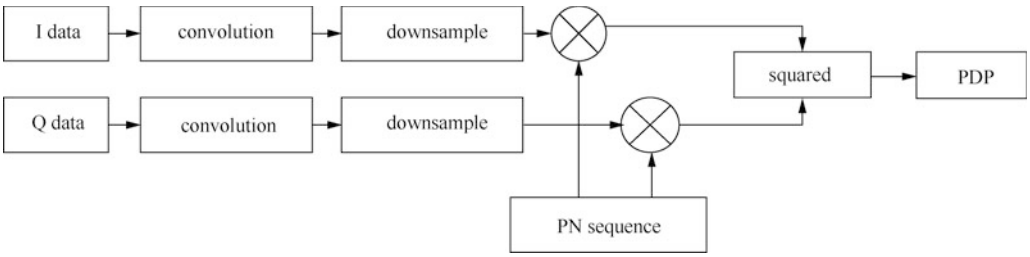

Figure 3 Data processing flow diagram

We used the least-squares method[12] to calculate the fitted path loss curves.

In the most general case, path loss is assumed to have a linear dependence with logarithmic distance, expressed as

$$PL(d) = \alpha + \beta \times 10\lg(d) + X_\sigma , \quad (1)$$

where $PL(d)$ is the path loss over the transmitter and receiver distance d in dB, α is the intercept, β is the path loss exponent, and X_σ is the shadow fading.

According to the least-square method, we can obtain the path loss exponent as

$$\beta = \frac{\sum_i^n (d_i - \overline{d}) \times (PL_i - \overline{PL})}{\sum_i^n (d_i - \overline{d})^2}, \quad (2)$$

and the floating intercept as

$$\alpha = \overline{PL} - \beta \times \overline{10\lg(d)} . \quad (3)$$

In the data processing, we used the least-squares method and the path loss based on close-in reference distance, which can be expressed as

$$PL(d) = PL(d_0) + 10n\lg\left(\frac{d}{d_0}\right) + X_\sigma , \quad (4)$$

where $PL(d)$ is the path loss over the transmitter and receiver distance d in dB, n is the path loss exponent, and X_σ is the shadow fading with mean 0, standard variance σ. λ is the wavelength, d_0 = 1 m; $PL(d_0)$ is the path loss under close-in reference distance, and can be expressed as

$$PL(d_0) = 20\lg\left(\frac{4\pi d_0}{\lambda}\right) . \quad (5)$$

From the above method, we obtain the PDP and then we carry the appropriate sum to obtain the received power.

3.2 Data analysis and results

At each distance, the transmitting antenna elevation angle was changed from −5° to 0° to 5°, corresponding to each elevation angle, and the receiving antenna azimuth angle changed from 0°and 360° in 5° steps. For the 0° elevation angle, the path loss is calculated as a function of Tx-Rx distance. The shadow fading is shown to meet the normal distribution. The fitted curves and cumulative distribution functions of shadow fading are shown in Fig.4 and the results are shown in Tab.3.

Fig.4(b) clearly shows that the shadow fading closely matches the Gaussian distribution. In Fig.4(a), the red diamond represents the minimum path loss under different horizontal angles in each distance, and the long red dashed line is the fitted curve corresponding to the path loss. The path loss exponent is 1.915 5, and the shadow fading standard deviation is 3.521 1 dB. The asterisk represents the total path loss under different horizontal angles in each distance, and the short blue dashed line is the fitting curve corresponding to the path loss. The path loss exponent is 2.320 4 and the shadow fading standard deviation is 7.590 5 dB.

Fig.5 shows that the received power in dBm varies with the azimuth angle under different elevation angles. It is clear that when the elevation angle is 0°,

the received power is approximately 3 dB larger than at other elevation angles. The received power values at −5° and 5° are close to consistent.

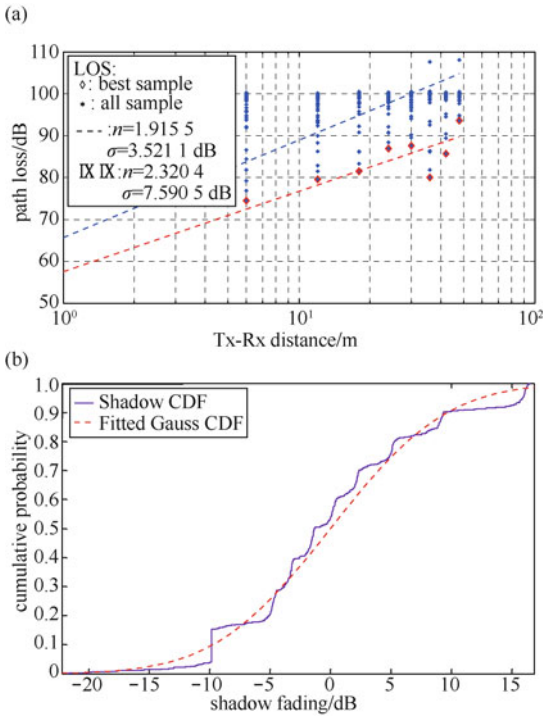

Figure 4 Results of path loss measurement: (a) Path loss fitted curves; (b) The cumulative distribution function of the shadow fading

Table 3 Results of path loss parameters

analysis method	n	σ/dB
all Samples	2.320 4	7.590 5
best Sample	1.915 5	3.521 1

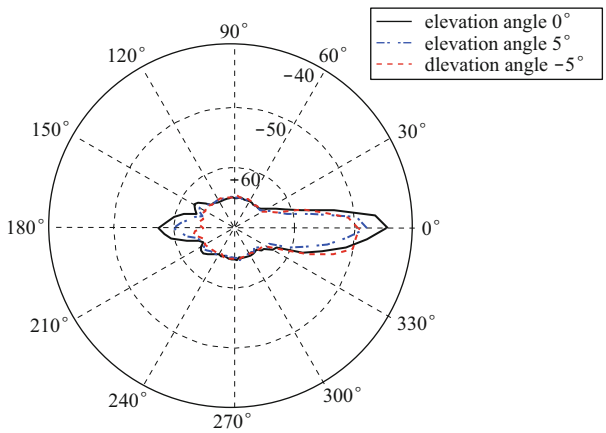

Figure 5 Angle spectrum

The proposed method is based on the close-in reference distance; if not, the path loss exponent is 0.280 5, and the shadow fading standard variance is 4.140 8 dB. On this issue, we hope the relevant scholars discuss with us.

Fig.6 shows the PDP of the LOS and NLOS scenarios, and it is clear that the multi-path distribution is not very obvious; this may be related to the long and narrow corridor test environment.

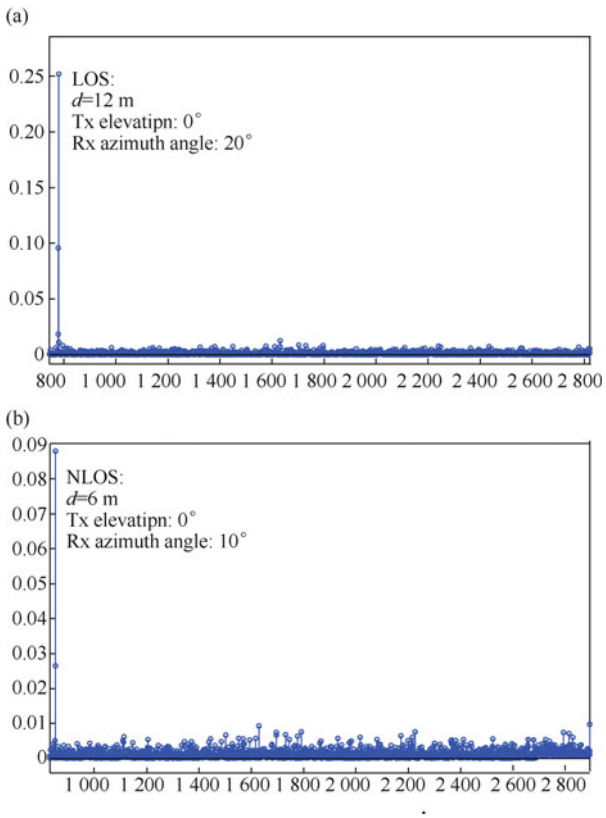

Figure 6 Results of PDP: (a) PDP of LOS scenario; (b) PDP of NLOS scenario

4 Conclusion

To understand the characteristics of the high-frequency band, i.e. 15 GHz, for future research and development of 5G communication technologies, in this study we conducted extensive measurements on this band in an indoor corridor environment. A testing system was built, and through data processing and

modeling, we obtained the path loss exponent n as 2.320 4. The shadow fading effect is shown to follow the Gaussian distribution with standard variance of 7.590 5 dB. Moreover, in this study, we analyzed the received power under different transmitting antenna elevation angles, and determined that the propagation performance is better when the elevation angle is 0°. Our work can be regarded as a reference for technology research and network planning in the next generation of mobile communication.

References

[1] ITU. Radio Regulations (Edition of 2012)[EB/OL]. http://www.itu.int/pub/R-REG-RR-2012.

[2] CHOI M S, GROSSKOPF G, ROHDE D. Statistical characteristics of 60 GHz wideband indoor propagation channel[C]//IEEE 16th International Symposium on Personal, Indoor and Mobile Radio Communications, 2005, 1: 599-603.

[3] XU H, KUKSHYA V, RAPPAPORT T S. Spatial and temporal characteristics of 60-GHz indoor channels[J]. IEEE journal on selected areas in communications, 2002, 20(3): 620-630.

[4] Smulders P F M, Wagemans A G. Wideband indoor radio propagation measurements at 58 GHz[J]. Electronics letters, 1992, 28(13): 1270-1272.

[5] GENG S, KIVINEN J, ZHAO X, et al. Millimeter-wave propagation channel characterization for short-range wireless communications[J]. IEEE transactions on vehicular technology, 2009, 58(1): 3-13.

[6] FU W, HU J, ZHANG S. Frequency-domain measurement of 60 GHz indoor channels: a measurement setup, literature data, and analysis[J]. IEEE instrumentation & measurement magazine, 2013, 16(2): 34-40.

[7] HAKEM N, DELISLE G, COULIBALY Y. Radio-wave propagation into an underground mine environment at 2.4 GHz, 5.8 GHz and 60 GHz[C]//The 8th European Conference on Antennas and Propagation, 2014: 3592-3595.

[8] ANDERSON C R, RAPPAPORT T S. In-building wideband partition loss measurements at 2.5 and 60 GHz[J]. IEEE transactions on wireless communications, 2004, 3(3): 922-928.

[9] GHASSEMZADEH S S, JANA R, RICE C W, et al. A statistical path loss model for in-home UWB channels[C]//IEEE Conference on Ultra Wideband Systems and Technologies, 2002: 59-64.

[10] SAMIMI M K, RAPPAPORT T S. Ultra-wideband statistical channel model for non line of sight millimeter-wave urban channels[C]//2014 IEEE Global Communications Conference, 2014: 3483-3489.

[11] BOHDANOWICZ A, JANSSEN G J M, PIETRZYK S. Wideband indoor and outdoor multipath channel measurements at 17 GHz[C]// Vehicular Technology Conference, 1999, 4: 1998-2003.

[12] MACCARTNEY G R, ZHANG J, NIE S, et al. Path loss models for 5G millimeter wave propagation channels in urban microcells[C]// IEEE Global Communications Conference, 2013: 3948-3953.

About the authors

XU Hui was born in 1976. He received the M.E. degree in 2004 from Shanghai Jiao Tong University. He is now a senior engineer in Shanghai Institute of Microsystem and Information Technology, Chinese Academy of Sciences and Shanghai Research Center for Wireless Communications. His research interest is the wireless communication networks. (Email: hui.xu@wico.sh)

ZHANG Wuxiong received the Ph.D. degree in 2013 from Shanghai Institute of Microsystem and Information Technology, Chinese Academic of Sciences. He is currently an assistant professor at SIMIT and Shanghai Research Center for Wireless Communications. His research interests include 4G/5G mobile communication systems and vehicular networks.

YANG Yang was born in 1974. He received the Ph.D. degree in 2002 from the University of Hong Kong. He is now a professor in Shanghai Institute of Microsystem and Information Technology, Chinese Academy of Sciences and Shanghai Research Center for Wireless Communications. His research interest is the wireless ad hoc and sensor networks.